THE JOURNAL OF BIOLOGICAL CHEMISTRY VOL. 289, NO. 28, pp. 19778–19788, July 11, 2014

ORA1, a Zebrafish Olfactory Receptor Ancestral to All Mammalian *V1R* Genes, Recognizes 4-Hydroxyphenylacetic Acid, a Putative Reproductive Pheromone

Received for publication, April 10, 2014 Published, JBC Papers in Press, May 15, 2014, DOI 10.1074/jbc.M114.573162

Maik Behrens[‡], Oliver Frank[§1], Harshadrai Rawel[¶1], Gaurav Ahuja[‖1], Christoph Potting[‖], Thomas Hofmann[§], Wolfgang Meyerhof[‡], and Sigrun Korsching[‖2]

From the [‡]Department of Molecular Genetics, German Institute of Human Nutrition Potsdam-Rehbruecke, Arthur-Scheunert-Allee 114-116, 14558 Nuthetal, the [§]Chair of Food Chemistry and Molecular Sensory Science, Technische Universität München, Lise-Meitner-Strasse 34, 85354 Freising, the [¶]Institute of Nutrition Science, University of Potsdam, Arthur-Scheunert-Allee 114-116, 14558 Nuthetal, and the [‖]Institute of Genetics, University at Cologne, Zülpicher Str. 47A, 50674 Cologne, Germany

Background: No ligands are known for any olfactory receptor of the *v1r*-related *ora* gene family.
Results: Zebrafish ORA1 recognizes with high sensitivity and specificity 4-hydroxyphenylacetic acid. This compound elicits oviposition behavior.
Conclusion: ORA1 was deorphanized with a ligand that may be a reproductive pheromone.
Significance: Pheromone reception conceivably might be the ancestral function of the *ora*/v1r family.

The teleost *v1r*-related *ora* genes are a small, highly conserved olfactory receptor gene family of only six genes, whose direct orthologues can be identified in lineages as far as that of cartilaginous fish. However, no ligands for fish olfactory receptor class A related genes (ORA) had been uncovered so far. Here we have deorphanized the ORA1 receptor using heterologous expression and calcium imaging. We report that zebrafish ORA1 recognizes with high specificity and sensitivity 4-hydroxyphenylacetic acid. The carboxyl group of this compound is required in a particular distance from the aromatic ring, whereas the hydroxyl group in the *para*-position is not essential, but strongly enhances the binding efficacy. Low concentrations of 4-hydroxyphenylacetic acid elicit increases in oviposition frequency in zebrafish mating pairs. This effect is abolished by naris closure. We hypothesize that 4-hydroxyphenylacetic acid might function as a pheromone for reproductive behavior in zebrafish. ORA1 is ancestral to mammalian V1Rs, and its putative function as pheromone receptor is reminiscent of the role of several mammalian V1Rs as pheromone receptors.

Pheromones play essential roles in many intraspecies communications, from mating preferences to control of aggression and individual recognition. Chemical signaling also occurs between species, *e.g.* for prey or predator detection. In mammals two large gene families are thought to be mainly responsible for detection of these signals, vomeronasal receptors type 1 and type 2 (V1R and V2R).[3] V2R receptors have been shown to recognize peptides (1, 2), whereas V1R ligands are found among low molecular weight molecules, such as steroids (Refs. 3 and 4, see also Ref. 5). We have recently shown that a small and highly conserved olfactory receptor gene family of just six *ora* genes (6) constitutes the ancestral repertoire, from which the large and dynamically evolving mammalian *v1r* families originate. All mammalian *v1r* genes are monophyletic with a single pair of *ora* genes, *ora1* and *ora2* (6), whose direct orthologues are present already in cartilaginous fish (7). In the light of such drastic differences in evolutionary characteristics for *v1r* and *v1r*-related *ora* genes it would be interesting to compare ORA ligands to those found for V1Rs. It is conceivable that ligands of the slowly evolving *ora* genes could be closer to those of ancestral *v1r* genes than the ligands of contemporary, rapidly evolving *v1r* genes themselves.

The zebrafish olfactory system is well characterized (Ref. 8 and references therein), and so we chose zebrafish *ora* genes for cloning and expression in a mammalian cell line. Activation of the receptors was analyzed by calcium imaging, using a variety of plausible assumptions as to potential ligands. Although none of these assumptions were borne out, eventually one led us on the track for a high affinity ligand of ORA1. We report the structure-activity tuning of ORA1, and show that the most effective ligand, 4-hydroxyphenylacetic acid, modulates reproductive behavior of zebrafish.

EXPERIMENTAL PROCEDURES

Cloning of Zebrafish ORA1 and ORA2 cDNA—*ora1* and *ora2* are monoexonic genes, whose full-length coding sequences were amplified from zebrafish genomic DNA, using the following primers: ORA1_FW 5′-TAGAATTCATGGACCT-GTGTGTCACCA-3′, ORA1_RV 5′-ATAGTTTAGCGGCCG-CCGTTCTTGCCGCTGGAGTT-3′, ORA2_FW 5′-CGGAAT-TCATGATTGCGGAGG-CTGTG-3′, ORA2_RV 5′-ATA-GTTTAGCGGCCG-CCGTGCATGGTCTCTGGCTG-3′. Forward primers contain a 5′ EcoRI site and reverse primers contain a NotI site. After PCR amplification, reaction products were digested with EcoRI and NotI, and cloned into the EcoRI and NotI sites of the modified vector pcDNA5FRT PM (9), thereby adding an amino-terminal sst3 epitope to facilitate effi-

[1] These authors contributed equally to this article.
[2] To whom correspondence should be addressed. Tel.: 49-221-470-4843; Fax: 49-221-470-5172; E-mail: sigrun.korsching@uni-koeln.de.
[3] The abbreviations used are: V1R and V2R, vomeronasal 1 receptor and vomeronasal 2 receptor.

cient cell surface localization and a carboxyl-terminal HSV (herpes simplex virus glycoprotein D) tag to enable immunological detection of the receptors.

Immunocytochemistry of ORA Constructs Transfected into HEK 293 Cells—Immunocytochemical detection of HEK 293T cells stably expressing the G protein-chimera Gα16gust44 was mainly done as described previously (10). Briefly, cells were seeded onto poly-D-lysine-coated glass coverslips in 24-well plates. Cells were transiently transfected with constructs coding for ORA1 or ORA2 using Lipofectamine 2000 (Invitrogen), and incubated for 24 h at 37 °C in 5% CO_2. Next, the cells were washed twice with PBS and placed for 30 min on ice to block endocytosis. For cell surface labeling biotinylated concanavalin A (Sigma) was applied at a dilution of 1:2,000 (1 h on ice). Repetitive washing with ice-cold PBS was followed by methanol/actone fixation (1:1 (v/v)) for 2 min. Following washing with PBS at room temperature, cells were incubated with 5% normal horse serum in PBS. Receptor proteins were detected with a 1:15,000 diluted anti-HSV antibody applied for 1 h at room temperature in blocking reagent (5% normal horse serum in PBS). Excess antibodies were removed by washing with PBS, before 1:2,000 diluted anti-mouse Alexa 488 and 1:1,000 diluted streptavidin Alexa 633 in PBS + 5% normal horse serum was applied for 1 h at room temperature. Finally, the glass coverslips were washed three times with PBS, once with deionized H_2O, and mounted with DAKO fluorescent mounting medium (DAKO). Images were taken by confocal laser scanning microscopy (Leica TCS SP2). For determination of expression rates 3 representative images per construct were taken and the number of green (= receptor expressing) and red (= total cell number) cells were counted.

Functional Calcium Imaging Experiments—The functional calcium imaging experiments were performed according to Ref. 10. Briefly, HEK 293T cells stably expressing the G protein-chimera Gα16gust44 were seeded onto 96-well plates coated with 10 μg/ml of poly-D-lysine. The next day cells were transiently transfected with ORA1, ORA2, or human bitter taste receptor TAS2R16 constructs using Lipofectamine 2000 (Invitrogen). After 24 h the cells were washed with buffer C1 (130 mM NaCl, 5 mM KCl, 10 mM Hepes, pH 7.4, 2 mM $CaCl_2$, 10 mM glucose), and loaded with the calcium-responsive dye Fluo-4 AM in the presence of 1 mM probenecide, an inhibitor of ABC transporter A1. To remove excessive fluorescence dye, cells were washed three times with buffer C1 and transferred into a fluorometric imaging plate reader (FLIPR, Molecular Devices) for measurement. Test substances were dissolved in C1 buffer and the changes in fluorescence after application of test substances were monitored. For the calculation of dose-response functions data from at least two independent experiments were obtained. For each experiment the signals of triplicate wells for each concentration were averaged and the corresponding fluorescence changes of mock-transfected cells were subtracted. Graphs and calculations of EC_{50} concentrations were performed using SigmaPlot. For the EC_{50} value determination nonlinear regression analysis was performed using the equation: $f(y) = (a - d)/1 + (x/EC_{50})^{nh} + d$.

Oxidation of L-Tyrosine and Related Compounds with Hydrogen Peroxide—To determine whether oxidative processes have resulted in the formation of agonistic compounds originating from "aged" L-tyrosine, we incubated candidate substances with hydrogen peroxide solution. 100 mg of freshly ordered L-tyrosine proved to be inactive on ORA1-transfected cells in functional calcium imaging experiments, as well as the same amount of L-dopamine and L-phenylalanine were mixed with 250 μl of 30% hydrogen peroxide solution (because of limited solubility 600 μl were used for L-phenylalanine) and incubated for several hours at room temperature. After this, the samples were subjected to brief centrifugation, the supernatants were diluted at least 10,000-fold and then taken for subsequent functional analyses. The remaining H_2O_2 (at most 1 mM or 0.003%) had no effect by itself.

HPLC Purification of Aged L-Tyrosine—Both analytical and preparative RP-HPLC of the samples was performed on a PRONTOSIL 120-3-C18, SC 150-ace-EPS column (150 × 4.6 mm, 3 μm; Bischoff Analysentechnik und -geraete GmbH, Leonberg, Germany) using a flow rate of 0.8 ml/min, UV detection at 280 nm, and a column temperature of 25 °C with a JASCO (Labor und Datentechnik GmbH, Gross-Umstadt, Germany) chromatographic system. The separation is based on the hydrophobic interactions of the analytes with the reverse phase filling of the column. A distilled water (acidified with 2% acetic acid; v/v)/methanol gradient was applied under the following conditions: 0–20% methanol, 2 min; 20–35% methanol, 18 min; 35–68% methanol, 2 min; 68% methanol, 3 min; 0–68% methanol, 3 min; 0% methanol, 12 min (regeneration/equilibration). The tyrosine samples (10 mg/ml) were dissolved in distilled water. The concentration was decreased in case of analytical HPLC. The injection volume of the samples was 10–20 μl. Altogether 10 fractions were collected. Fraction 2 was identified to contain pure tyrosine using an external standard and HPLC-MS (Shimadzu chromatographic LC-10 system equipped with a mass spectrometer LC-MS 2010 EV, Kyoto, Japan; MS conditions were as follows: Interface ESI, CDL temperature/heating block = 230 °C, nebulizing gas flow = 1.5 ml/min; detector voltage = 1.7 kV; interface voltage = 4.5 V; CDL voltage = 0. = V; Q-array voltage, DC = 20–30V, R_F = 85–125 V; scan modus, event time = 0.8 s, m/z = 120–550) performed under the same separation conditions as described above. The compound in fraction 6 could not be ionized under the applied MS conditions. The total peak area of the fractions was used to estimate the amount in fractions 2 and 6 using an external tyrosine standard. The relative composition was determined to be 67.6 and 5.2%, respectively.

Nuclear Magnetic Resonance (NMR) Spectroscopy—One- and two-dimensional ^1H and ^{13}C NMR spectra were acquired on a 500 MHz Avance III spectrometer (Bruker, Rheinstetten, Germany), respectively. Dimethyl sulfoxide-d_6 MeOD (9:1, v/v) was used as solvent and chemical shifts are reported in parts per million relative to the solvent signal. Homo- and heteronuclear correlation experiments were carried out using the pulse sequences taken from the Bruker software library. Data processing was performed by using TopSpin (2.1; Bruker, Rheinstetten, Germany) as well as Mestre-C (Mestrelab Research, A Coruña, Spain).

Behavioral Assays—Analysis of aversion or attraction was performed as described (11). Individual adult zebrafish (Ab/Tü strain, 6–8 months old) were tested in an elongated tank (10 × 100 cm, 9 liters fresh filtered water) after 45 min of habituation. Fish movements were video recorded (30 frames/second) from the side for 5 min before and after stimulus addition (180 μl of odor or tank water as control) by an experimenter not visible to the fish. Fish movements were video recorded for 5 min before and after stimulus addition (180 μl of 1 mM 4-hydroxyphenylacetic acid or water) and tracked using LoliTrack version 3 automated motion tracker (12). Distance to the odor source and velocity were determined using Open Office (Apache). Mean displacement was calculated as a difference of average location and expressed as percent of total tank length. Significance was evaluated by Student's *t* test (two-sided, unpaired).

To examine oviposition (egg laying), zebrafish were kept gender-separated for 1–2 weeks prior to the experiment. In the evening preceding the experiment the breeding pairs were gently transferred to breeding tanks (20 × 10 cm, 600 ml of water), with female and male separated by a translucent divider. The next morning, one-half hour into the light cycle the divider was removed allowing the fish free movement. Pairs without eggs after the 90-min contact time were then supplemented with various concentrations of 4-hydroxyphenylacetic acid in 10 mM Tris, pH 7.4, or with buffer alone. The pairs were monitored for the presence of eggs 90 min after the stimulus. For generation of transiently anosmic fish, both nostrils were glued with Histoacryl® (Braun) and the fish were allowed a resting period of 24 h before being tested. Anosmic fish showed normal motility. Significance was estimated by χ-square analysis.

RESULTS

ORA1 and ORA2 Are Efficiently Expressed and Localize to the Plasma Membrane—We have chosen zebrafish as the species to search for ORA1/ORA2 agonists, because in this species the expression of all *ora* family members in olfactory sensory neurons has been shown (6). For heterologous expression we selected a system that has been very efficient for functional expression of bitter taste receptors (13), which are the closest homologues of the *ora*/*v1r* family (6). In short, the full-length receptor sequence is fused to an N-terminal sst3 tag serving as signal sequence (14) and a C-terminal hsv-epitope to enable detection (15). The constructs were transiently expressed in HEK 293T cells stably transfected with the broadly reactive G protein, Gα16gust44 (16, 17). G protein-coupled chemoreceptors are sometimes poorly transported to the plasma membrane in heterologous systems (see Refs. 18–20), and we therefore analyzed the intracellular distribution of ORA1/ORA2 by immunocytochemical detection. The receptors were visualized using an antibody against the C-terminal hsv-epitope and the cell surface was stained by concanavalin A, which serves both as general cell marker and as label for plasma membrane (for details see "Experimental Procedures").

Both ORA receptors are robustly and reproducibly expressed. Nearly two-thirds of all cells express each receptor (Fig. 1*A*), and a large fraction of the expressed protein appears to be localized at the level of the plasma membrane as seen by the superposition of the receptor signals with those of the cell surface label (Fig. 1*A*). Thus, an essential prerequisite for functional characterization is fulfilled for both ORA1 and ORA2.

ORA1 but Not ORA2 Reacts to a Mixture of Amino Acids—Previous studies have demonstrated that amino acids and pheromones represent preferred olfactory stimuli for fish (21–23). We have tested both types of potential ligands, using as positive control cells expressing the bitter taste receptor TAS2R16 stimulated with the bitter compound D-(−)-salicin (9). None of the pheromones tested, among them those known to activate some zebrafish glomeruli (21), could activate either ORA1 or ORA2 (Table 1).

In contrast, the mixture of all 20 proteinogenic L-amino acids elicited a strong calcium signal for ORA1-transfected cells at 1 mM concentration per amino acid with a time course resembling that of the positive control (Fig. 1*B*). Stimulation of transfected cells with buffer alone had no effect, and likewise stimulation of mock-transfected cells (empty expression vector) with the full 20 amino acid mixture elicited no response (Fig. 1*B*). Thus the signal obtained for ORA1 appears to be a specific receptor-mediated response to the amino acid mixture. Ora2-transfected cells were not activated by the mixture (Fig. 1*B*).

ORA1 Activation Is Caused by a L-Tyrosine Contaminant—To identify which of the 20 L-amino acids are able to activate ORA1, we next separately used each of the amino acids at the same concentration (1 mM) (Fig. 1*C*). Only one amino acid, tyrosine, mimicked the response elicited by the mixture of amino acids, whereas the other 19 amino acids had no effect (Fig. 1*C*), suggesting that ORA1 activation in the previous experiment had been solely due to the presence of the L-tyrosine reagent.

However, when we attempted to validate this result using other lots of tyrosine we did not observe any activation of ORA1 (Fig. 2*A*). This excludes L-tyrosine as ligand and suggests a contaminant as the active compound. Because the first, active lot had aged for a prolonged period at +4 °C and indeed exhibited an off-color, we suspected contamination by some degradation product as the active ingredient, which presumably was only present in trace amounts and therefore likely to be a high potency agonist.

The Active Compound Is Generated by Oxidation of Tyrosine—We first examined whether the active ingredient might have formed by oxidation of tyrosine, a process expected to happen upon prolonged storage. We reacted fresh L-tyrosine with 30% hydrogen peroxide and tested the reaction product at different dilutions. Indeed, even at 1:10,000 dilution a strong signal was generated, similar to the signal elicited by the aged tyrosine lot (Fig. 2*A*), and in stark contrast to the complete inability of the fresh tyrosine itself to activate ORA1 (Fig. 2*A*). When the closely related substances L-dopamine and L-phenylalanine were subjected to the same oxidation procedure, no response was elicited either for the fresh (Table 1) or the oxidized compounds (Fig. 2*A*). Furthermore, hydrogen peroxide by itself had no effect (Fig. 2*A*). The outcome of this experiment suggested that the active substance in the aged L-tyrosine indeed originated from oxidation of L-tyrosine.

Purification and Identification of the Active Compound by HPLC and LC-MS—To identify the active compound or compounds, we first performed an analytical HPLC separation of

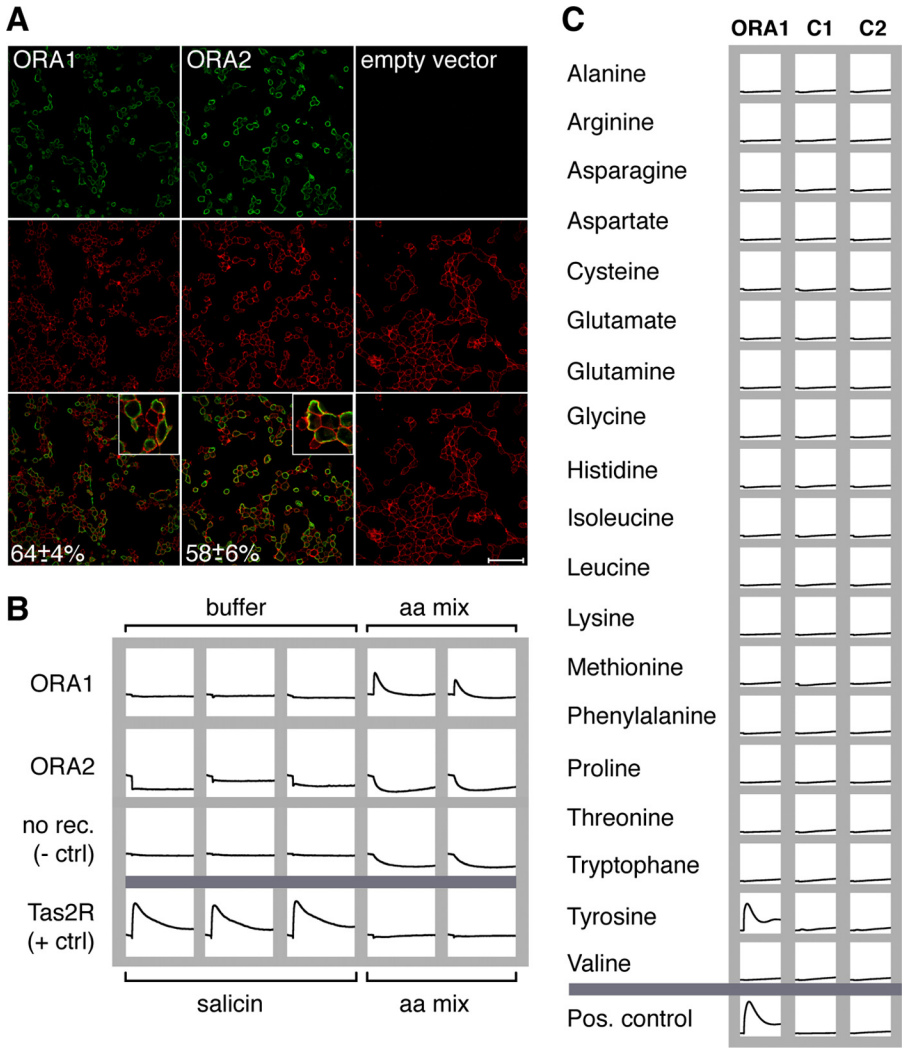

FIGURE 1. **Activation of ORA receptors by amino acids.** *A,* ORA receptors localize to the plasma membrane. HEK 293T cells were transfected as indicated, and receptor protein was detected with an antibody against the C-terminal HSV epitope and Alexa 488-coupled secondary antibody (*green*, *upper row*). Cell surfaces are visualized using biotinylated concanavalin A in combination with streptavidin/Alexa 633 (*red label*, *middle row*). *Yellow* color in the overlay (*bottom row*) indicates close proximity of receptors with the plasma membrane. *Insets* show groups of cells magnified by a factor of three. Note the absence of green signals in cells transfected with empty vector (*third column*). Cells expressing the *ora* genes (*green*) were counted and expressed as percentage of total cells (*red*) ± S.D. *Scale bar*, 75 μm. *B,* ORA1 but not ORA2 is activated by an amino acid mixture. HEK 293T cells were transiently transfected with ORA1, ORA2, TAS2R16, or empty vector, loaded with Fluo-4 AM, and stimulated with a mixture of all 20 proteinogenic amino acids (final concentration 1 mM each). Changes in calcium levels were analyzed in a fluorometric imaging plate reader. Only ORA1-transfected cells show a response, comparable in size to that of the positive control (TAS2R16 and 10 mM of the agonist D-(−)-salicin (9)). Thus, ORA1 appears to be specifically activated by one or several amino acids present in the amino acid mixture. *C,* ORA1-expressing cells only respond to tyrosine. HEK 293T cells were transiently transfected with ORA1 or empty vector, loaded with the calcium-sensitive dye fluo-4 AM, and analyzed in a fluorometric imaging plate reader before and after application of single amino acids at 1 mM concentration each. Duplicate wells, one of which is shown here, were tested for each experimental condition. No change in fluorescence was seen for untransfected cells (*middle column*) or cells transfected with empty vector (*right column*). The ORA1 response to tyrosine is comparable in size and time course to that of the bitter taste receptor TAS2R16 to a strong agonist (D-(−)-salicin, 10 mM (9)).

aged tyrosine using a water/methanol gradient for elution from a reversed phase C_{18} column (Fig. 2*B*, for details see "Experimental Procedures"). Ten major peaks were collected, dried down, re-dissolved in 200 μl of H_2O, and tested at 1:6 dilution by functional calcium imaging of ORA1-expressing cells (Fig. 2*C*). ORA1 was activated by a single peak contained in fraction 6, and no signals were observed in all other factions, consistent with a single compound underlying the observed activation by aged tyrosine. Fraction 6 amounted to 5.2% of the total peak area, *i.e.* it constitutes a minor component of aged tyrosine.

To obtain enough material for structure determination the HPLC purification was scaled up to obtain about 10 mg of purified fraction 6. The exact mass was determined by LC-TOF/MS resulting in an elemental composition of $C_8H_8O_3$. LC-MS revealed an intense pseudo molecular ion $[M\text{-}H]^-$ with m/z 151.0 and additional LC-MS/MS experiments showed a daughter ion m/z 107.0, supporting the cleavage of a molecule of CO_2, *i.e.* the presence of a carboxylic group. Analysis of the ^1H NMR spectroscopic data showed a total of 3 resonance signals, two of them aromatic (6.67 and 7.02 ppm) and all three signals resulting from 2 protons each. The aromatic protons showed the typical coupling pattern of an $AA'XX'$ spin system of a *para*-substituted aromatic ring. The third signal at 3.37 ppm was shown by DEPT-135 as well as heteronuclear single quantum coherence experiments to be derived from a methylene group. The complete assignment of the structure was achieved by

TABLE 1
Binding spectrum of ORA1

Active Compounds	*EC_{50} (μM)*	*Max. amplitude (ΔF/F)*
4-hydroxyphenylacetic acid	1.9 ± 0.3	0.86 ± 0.03
4-toloylacetic acid	14.8 ± 1.8	0.54 ± 0.03
3,4-methylenedioxyphenylacetic acid	16.0 ± 3.6	0.54 ± 0.04
4-methoxyphenylacetic acid	16.5 ± 2.7	0.39 ± 0.05
4-chlorophenylacetic acid	16.6 ± 1.6	0.49 ± 0.02
3,4-dihydroxyphenylacetic acid	22.8 ± 2.7	0.36 ± 0.02
Phenylacetic acid	30.5 ± 2.8	0.52 ± 0.01
4-aminophenylacetic acid	91.7 ± 17.3	0.58 ± 0.02
3-(4-hydroxyphenyl)-propionic acid	191.8 ± 39.8	0.17 ± 0.01
4-hydroxyphenylacetamide	199.9 ± 52.2	0.39 ± 0.03
Methyl-4-hydroxyphenylacetic acid	221.0 ± 25.2	0.45 ± 0.02

Inactive Compounds	*Maximal concentration tested (mM)*		
Proteinogenic amino acids			
L-alanine	1	L-leucine	1
L-arginine	1	L-lysine	1
L-asparagine	1	L-methionine	1
L-aspartate	1	L-phenylalanine	1
L-cysteine	1	L-proline	1
L-glutamate	1	L-serine	1
L-glutamine	1	L-threonine	1
Glycine	1	L-tryptophane	1
L-histidine	1	L-tyrosine	1
L-isoleucine	1	L-valine	1
Other amino acids and derivatives			
4-amino-L-phenylalanine	10	D-tyrosine	1
4-hydroxy-L-phenylglycine	10	DL-m-tyrosine	1
5-hydroxy-L-tryptophane	0.03	DL-o-tyrosine	3
4-iodo-L-phenylalanine	0.3	L-tyrosine methylester	1
4-nitro-L-phenylalanine	1		
Steroids and prostaglandins			
4-androstene-3,17-dione	0.003	15-keto-prostaglandin F2α	0.003
4-Pregnen-17,20β-diol-3-one	0.003	Prostaglandin F2α	0.003
4-Pregnen-17,20β-diol-3-one-20-sulphate	0.003		
4-Pregnen-17,20β,21-triol-3-one	0.003		
Other compounds			
L-DOPA	1	4-phenylenediacetic acid	1
Dopamine	1	Serotonin	0.3
4-hydroxybenzoic acid	3	Skatole	0.01
Indole	0.1	Tyramine	1
Indole-3-carboxylic acid	0.2		

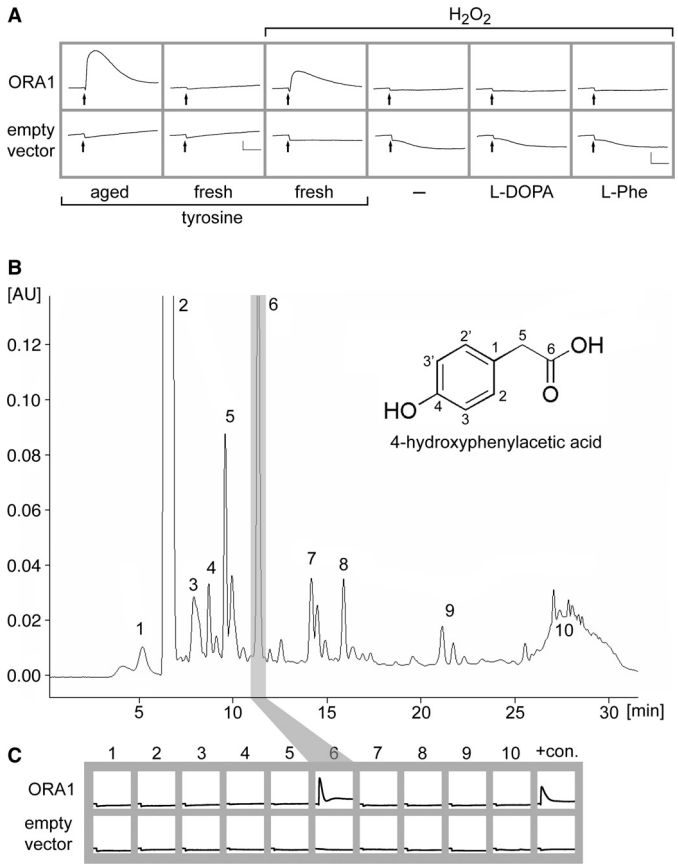

FIGURE 2. **ORA1 is activated by 4-hydroxyphenylacetic acid, a contaminant of aged tyrosine.** *A, top row*, cells were transfected with ORA1, and challenged with 100 μM of different stimuli as indicated. Calcium traces are averaged from 3 wells. Only aged tyrosine (*first column*), *i.e.* the tyrosine lot used in Fig. 1, and oxidized fresh tyrosine (*third column*) were active, but fresh tyrosine itself (*second column*) was not. Hydrogen peroxide itself, L-dopamine (L-*DOPA*), and L-phenylalanine (L-*Phe*) had no effect. *Bottom row*, cells transfected with empty vector showed no response to any of the stimuli. Shown are calcium traces averaged from 2 wells. Scaling: *y* axis = relative units, *x* axis = 1 min. *B,* a single active compound is detected in aged L-tyrosine. 100 μg of aged tyrosine was separated by HPLC fractionation using a water/methanol gradient with UV detection at 280 nm. Ten fractions corresponding to peak absorbance rates (labeled 1–10) were collected at the following time points during the run: *1*, 3.4–5.6 min; *2*, 6.0–6.9 min; *3*, 7.5–8.2; *4*, 8.2–9.2 min; *5*, 9.2–10.2 min; *6*, 10.7–11.5 min; *7*, 13.7–14.9 min; *8*, 15.5–17.4; *9*, 20.6–23 min; *10*, 25–29.5 min. *y* axis, absorbance units (*AU*); *x* axis, run time (min). *Inset of B*, chemical characterization of fraction 6 showed 4-hydroxyphenylacetic acid as the main compound. The carbon atoms of 4-hydroxyphenylacetic acid are labeled by arbitrary numbers to allow easy association with the following analytical, mass spectrometry, and NMR data that resulted in unambiguous identification: UV-visible (0.1% aqueous HCOOH)/MeOH; 6/4, v/v): λ_{max} = 228, 276 nm; LC/TOF-MS: $C_8H_8O_3$; LC/MS (ESI^-): 151.1 (100; $[M\text{-}H]^-$); ^1H NMR (500 MHz; dimethyl sulfoxide-d_6/MeOD; 9/1, v/v; COSY): δ 3.37 [s, 2H, H-C(**5**)], 6.67 [m, 2H, H-C(**3**,**3**′)], 7.02 [m, 2H, H-C(**3**,**3**′)]; ^{13}C NMR (125 MHz; dimethyl sulfoxide-d_6/MeOD; 9:1, v/v; DEPT-135, heteronuclear single quantum coherence, heteronuclear multiple bond correlation): δ 40.3 (CH_2, C(**5**)), 114.8 (CH, C(**3**, **3**′)), 125.6 (C, C(**1**)), 130.1 (CH, C(**2**, **2**′)), 155.8 (C, C(**4**)), 173.2 (C, C(**6**)). *C*, each of the collected fractions was dried, redissolved, and used to stimulate ORA1-transfected HEK 293T cells. Only fraction 6 resulted in fluorescence changes. *Last column*, 100 μM unpurified aged L-tyrosine served as positive control (+*con.*). Cells transfected with empty vector showed no response to any fraction. Scaling: *y* axis, arbitrary units; *x* axis 9 min.

means of heteronuclear multiple bond correlation optimized for $^{2,3}J_{C,H}$ couplings. As an example, the carbonyl group resonating at 173.2 ppm showed a correlation signal with the protons of the methylene group, indicating a -CH_2COOH configuration and the carbon C(5) of the latter showed a cross-peak with the aromatic ring protons H-C(2,2′) via a $^3J_{C,H}$ coupling,

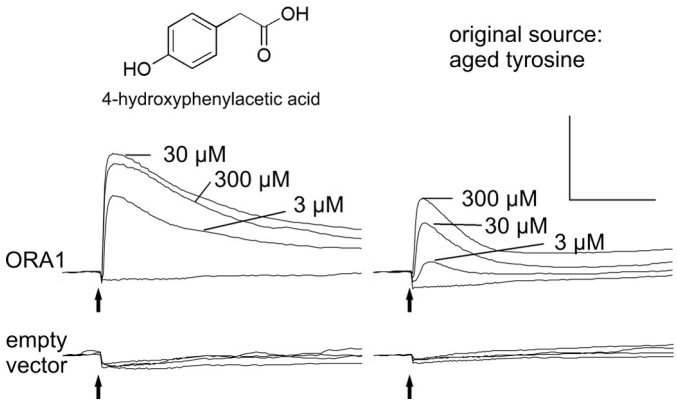

FIGURE 3. **Concentration-dependent saturable activation of ORA1 by 4-hydroxyphenylacetic *acid*.** HEK 293T cells transfected with ORA1 or empty vector were stimulated with different concentrations of 4-hydroxyphenylacetic acid, and calcium responses were imaged. For each concentration an average trace of three identically treated wells is shown (*left panel*). No response is seen for ORA1-transfected cells stimulated with buffer and for empty vector-transfected cells in all conditions (*bottom panels*). Note that ORA1-transfected cells are at least 10-fold more sensitive to 4-hydroxyphenylacetic acid than to aged tyrosine. *Scale bar*: *y* axis, arbitrary units; *x* axis, 2 min.

suggesting this acetyl group as ring substituent. The signal at 155.8 ppm is well in line with a quaternary carbon substituted in the *para*-position with a phenolic system and showed the expected correlations with protons H-C(2,2′) and H-C(3,3′), see Fig. 2*B* for nomenclature. Taking all spectroscopic data into consideration, the degradation product of L-tyrosine could be unequivocally identified as 4-hydroxyphenylacetic acid (Fig. 2*B*). Furthermore, spectroscopic data of commercially available 4-hydroxyphenylacetic acid showed an exact match with those of the fraction 6 compound.

Validation of 4-Hydroxyphenylacetic Acid as ORA1 Ligand—Calcium imaging of ORA1-transfected cells was performed with different concentrations of commercial 4-hydroxyphenylacetic acid in the 3–300 μM range. Responses were dose-dependent and saturated at 30 μM, at least an order of magnitude lower than the original source, aged tyrosine (Fig. 3). This ratio was consistent with the result from the HPLC separation, which showed that 4-hydroxyphenylacetic acid was a contaminant in the original source, well below 10%.

The absence of signals in cells transfected with empty vector (Fig. 3) attests to the specificity of the functional data for ORA1-transfected cells. From the results of all the functional experiments we concluded that 1) 4-hydroxyphenylacetic acid is a high potency agonist for the receptor ORA1, and 2) that relatively minor structural changes destroy the agonistic properties suggesting a pronounced selectivity of this receptor.

Activation of ORA1 by 4-Hydroxyphenylacetic-related Compounds—To better understand the molecular features required for ORA1 agonists, we measured dose-response relationships for a variety of compounds structurally related to 4-hydroxyphenylacetic acid (Fig. 4, Table 1). Among this group, no better agonist than 4-hydroxyphenylacetic acid was found, which remains by far the best agonist exhibiting the lowest threshold concentration (approximately 0.1 μM), the lowest EC_{50} concentration (1.9 $\pm$ 0.3 μM S.E.), and the largest maximal signal amplitude ($\Delta F/F > 0.8$).

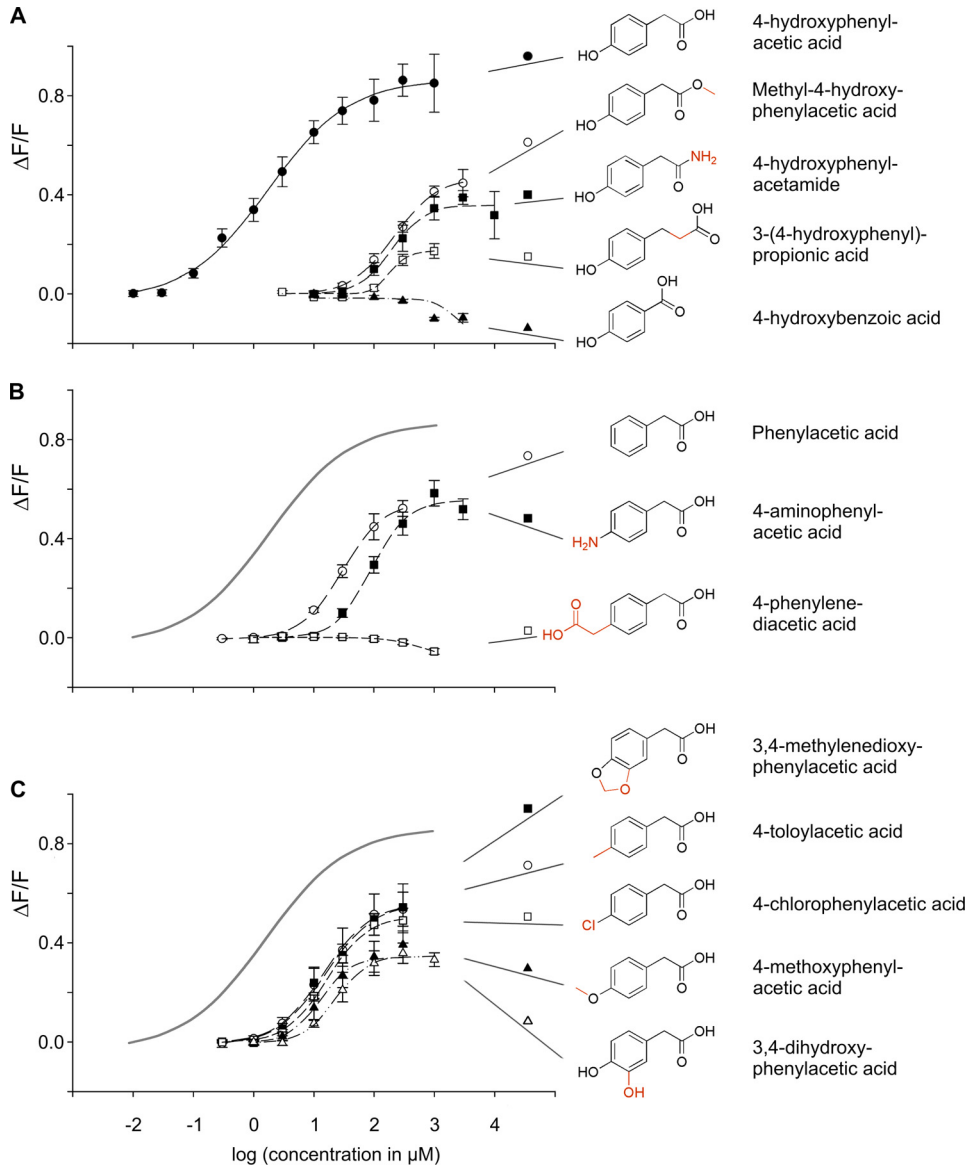

FIGURE 4. **Agonist selectivity and efficacy of ORA1.** HEK 293T Gα16gust44 cells were transfected with ORA1 cDNA and stimulated with increasing concentrations of compounds related to 4-hydroxyphenylacetic acid to monitor the corresponding dose-response functions. Resulting calcium signals were measured by fluorometric detection. *y* axis, $\Delta F/F$; *x* axis, decadic logarithm of the concentration given in micromolar. Structural formulas of the substances are shown to the *left* of their names. *A,* 4-hydroxyphenylacetic acid activates ORA1 with an EC_{50} value of 1.9 $\pm$ 0.3 μM and a maximal signal amplitude above 0.8 $\Delta F/F$. Structural alterations at the carboxyl group shift the dose-response curve to varying degrees to the *right* as well as reduce the maximal signal amplitude. *B*, structural alterations at the *para*-hydroxyl group shift the dose-response curve to the *right* as well as reduce the maximal signal amplitude. For comparison, the calculated dose-response curve for the optimal agonist, 4-hydroxyphenylacetic acid, is depicted in *gray*. *C,* 10-fold reduction in affinity by a positive inductive or mesomeric effect in *para*-position. For comparison, the calculated dose-response curve for the optimal agonist, 4-hydroxyphenylacetic acid, is depicted in *gray*.

Of 55 compounds tested, only 11 4-hydroxyphenylacetic acid-related compounds activated ORA1 and showed a dose-dependent response (Fig. 4, Table 1). The efficacy as estimated by the maximal signal amplitude of these compounds was clearly lower, maximally 60% of the value observed for 4-hydroxyphenylacetic acid (Table 1), suggesting that all represent partial agonists. The potency, as estimated by the EC_{50} value, varied about 100-fold, with that of 4-hydroxyphenylacetic acid about an order of magnitude higher than that of the next best agonists (Table 1). Interestingly, the potencies do not correlate well with maximal signal amplitudes (Table 1), suggesting that potency and efficacy can vary independently for this receptor.

The Carboxyl Group Is Required in a Particular Distance to the Aromatic Ring Structure—Amidation or methylation of the carboxyl group increases the EC_{50} value 100-fold, *i.e.* decreases the affinity by 2 orders of magnitude (4-hydroxyphenylacetamide and methyl-4-hydroxyphenylacetic acid, respectively, see Fig. 4*A*, Table 1). Slightly increasing the distance from the ring by intercalating a methylene group (3-(4-hydroxyphenyl)-propionic acid) reduces the affinity by the same amount, but in addition impairs the maximal signal amplitude massively, down to 0.1 $\Delta F/F$. Decreasing the distance of the carboxyl group from the ring abolishes the activity completely (4-hydroxybenzoic acid). Thus, the negative charge of the carboxyl group is

required at a particular distance from the ring for efficient binding and in particular signal transduction. This hypothesis is supported by our observation that many related compounds, which were completely unable to activate ORA1 (Table 1), show modifications in this part of the molecular structure, *e.g.* the addition of a charged group (4-hydroxy-L-phenylglycine).

The para-Hydroxy Group Is Not Absolutely Required—Omitting the *para*-hydroxy group (phenylacetic acid) results in about an order of magnitude reduced potency and only 60% of maximal signal amplitude (Fig. 4*B*, Table 1). However, many variations of the *para*-substituent reduce the potency more severely. For example, a negative mesomeric and inductive effect in the *para*-position by exchanging the hydroxyl group with an amino group (4-aminophenylacetic acid) leads to a 50-fold reduction in potency (Fig. 4*B*, Table 1). Introducing a bulky (and charged) substituent in the *para*-position eliminates the activity completely (4-phenylenediacetic acid, Fig. 4*B*).

A positive inductive or mesomeric effect at the *para*-position is only marginally better than omitting the *para*-substituent completely, as seen by the activities of 4-chlorophenylacetic acid, 4-toloylacetic acid, 3,4-methylenedioxyphenylacetic acid, 3,4-dihydroxyphenylacetic acid, and 4-methoxyphenylacetic acid (Fig. 4*C*, Table 1). Interestingly, all five compounds possess undistinguishable EC_{50} values (Table 1), suggesting that the exact shape and size of the *para*-substituent is not important. The latter two compounds exhibit reduced maximal signal amplitudes compared with the first three compounds (Fig. 4*B*, Table 1). This uncoupling of affinity and efficacy would be consistent with the *p*-substituent boosting the efficacy of the ligand. Taken together, the *para*-hydroxyl group is not required *per se* for activity, but enhances potency and efficacy massively.

4-Hydroxyphenylacetic Acid Modulates Zebrafish Reproductive Behavior—The high sensitivity of ORA1 for 4-hydroxyphenylacetic acid suggests that this compound might be a relatively close fit to the endogenous ligand, if not an endogenous ligand itself. Its potency is over 10-fold better compared with that of a recently identified ligand-receptor pair that signals aversion to decaying flesh (11). This would be consistent with ORA1 serving as pheromone receptor, which generally exhibit higher sensitivity than "normal" olfactory receptors (*cf.* Refs. 21 and 24). Thus, we embarked on a search for innate zebrafish behavior elicited by 4-hydroxyphenylacetic acid.

First, we investigated whether a point source of 4-hydroxyphenylacetic acid in a stationary tank would elicit attraction or avoidance behavior (11). For these experiments 180 μl of 4-hydroxyphenylacetic acid solution (1 mM) was added to the tank by an experimenter hidden from sight for the zebrafish. Using the identical setup the same ligand concentration has been found to elicit maximal aversion behavior for the above mentioned ligand/receptor pair with 10-fold lower affinity (*cf.* Fig. 5*B*). However, 4-hydroxyphenylacetic acid did not result in detectable attraction or avoidance behavior (Fig. 5, *A* and *B*). Furthermore, average velocity, a measure of agitation, did not change after a 4-hydroxyphenylacetic acid stimulus was given, and no incidents of freezing, a fear response, were observed (Fig. 5, *A* and *C*).

Second, we considered a possible function of 4-hydroxyphenylacetic acid as a signal in social interactions, and tested zebrafish pairs with 100 μM 4-hydroxyphenylacetic acid (final concentration). We noted chasing behavior and in one case oviposition after contact with the odor in the case of female/male pairs of zebrafish. This suggested to us that 4-hydroxyphenylacetic acid might be involved in regulation of reproductive behavior. It is well known that several reproductive hormones and their metabolites including prostaglandins and steroids and so far unidentified compounds do double duty as odors that signal the reproductive state of the female to the male and vice versa (see Ref. 22).

We then investigated a possible effect of 4-hydroxyphenylacetic acid on oviposition behavior by exposing pairs of female and male zebrafish to different concentrations of 4-hydroxyphenylacetic acid. Because pairing of zebrafish by itself can induce oviposition, we kept the pairs together for 90 min before stimulus or control solution was added. Under the experimental conditions used, this resulted in oviposition during the first 90 min in 5% of cases ($n = 66$). A similar frequency of 8% ($n = 25$) was observed for control pairs not exposed to stimulus during the next 90 min. This frequency was used as a conservative estimate of the background egg-laying frequency for the next 90 min. We report that oviposition frequency increased several-fold after addition of 100 μM (final concentration) 4-hydroxyphenylacetic acid. This increase was blocked after closing the nostrils of the female with tissue glue (Fig. 5*D*). Both the increase and the block were significant (χ square test, $n = 10$, $p < 0.001$, and $n = 7$, $p < 0.02$, respectively). The induced oviposition persists at 4-hydroxyphenylacetic acid concentrations of 30 and 10 μM (Fig. 5*D*), although the number of eggs laid appeared to decrease with decreasing concentration. The eggs appeared partially immature and contained a higher than normal percentage of opaque (dead) eggs. We hypothesize that this could be due to the 4-hydroxyphenylacetic acid stimulus occurring out of physiological context in our experimental situation. We conclude that 4-hydroxyphenylacetic acid at low concentrations can elicit a physiological response as part of a reproductive behavior repertoire.

DISCUSSION

Our deorphanization of ORA1 constitutes the first instance of a ligand identification for any member of the *ora* family of olfactor receptor genes. In fact, ORA1 is only the third deorphanized fish olfactory receptor overall, with the other two receptors belonging to other families (11, 25). The small family of just six *ora* genes is remarkable for its high degree of conservation and its rather constant family size, both different from all other olfactory receptor gene families analyzed so far. Furthermore, *ora* genes are under strong negative selection and teleost ORA receptors possess direct orthologs even in cartilaginous fish (7), *i.e.* before the evolutionary divergence in teleosts and tetrapods. Thus, the *ora* family is ancestral to the mammalian and more generally tetrapod *v1r* receptor gene repertoires. The *v1r* receptors form a monophyletic tree with two of the six *ora* genes, *ora1* and *ora2*. Therefore, fish *ora1* and *ora2* genes may remain closer to the ancestral *v1r* genes than the contemporary *v1r* genes themselves, which show a very dynamic evolution, and exhibit many gene birth and death events. We have therefore attempted deorphanization of zebrafish ORA1 and ORA2

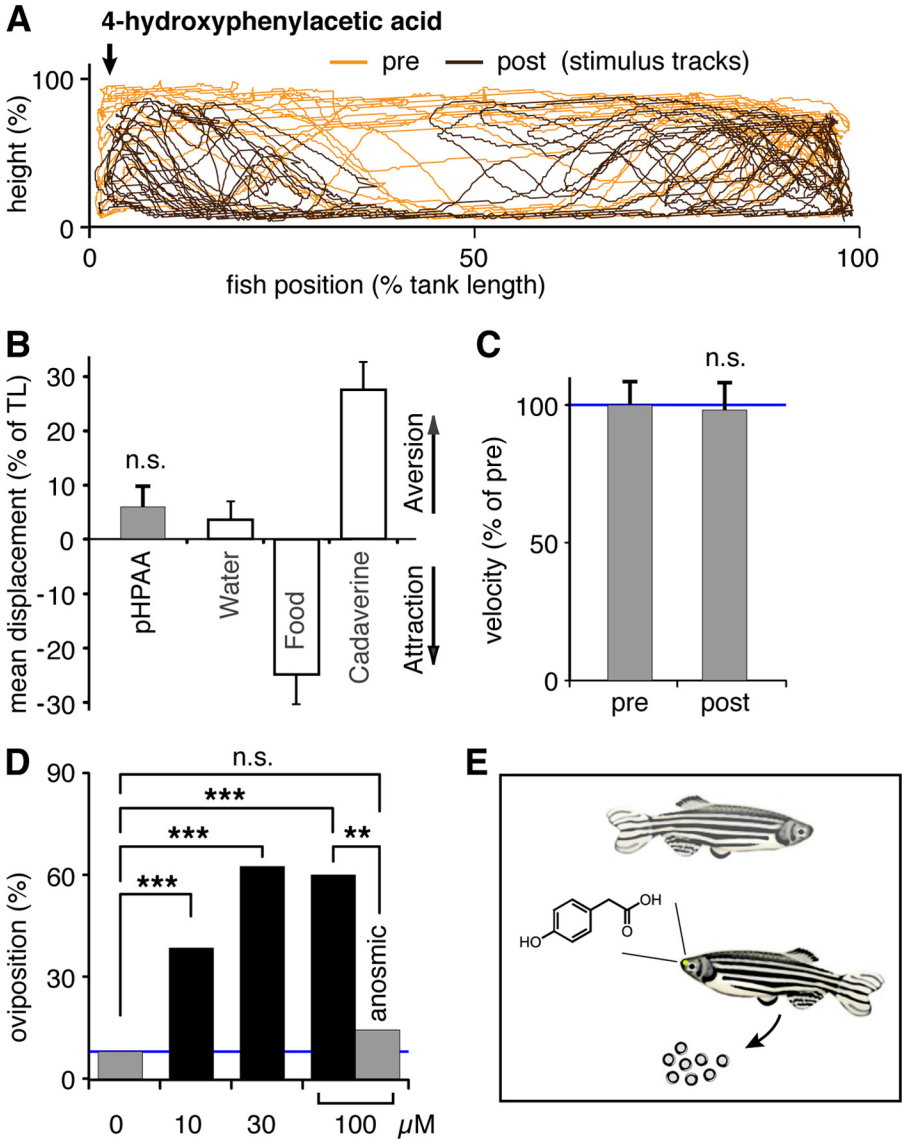

FIGURE 5. **Zebrafish behavioral responses to 4-hydroxyphenylacetic acid.** *A,* fish were exposed to a point source (*arrow*) of 4-hydroxyphenylacetic acid (1 mM), and their movements were video tracked 5 min before and after stimulus addition. A representative track is shown, *orange*, prestimulus; *brown*, post-stimulus. *B,* quantitative evaluation of tracks shows no evidence for attraction or aversion by 4-hydroxyphenylacetic acid (*pHPAA*), *n.s.*, not significant. For comparison, attraction by food extract (*food*) and aversion to cadaverine is shown, raw data for these panels, see Ref. 11. *C,* no difference in motility was seen after exposure to 4-hydroxyphenylacetic acid. Motility is measured as average velocity and expressed as percent of the prestimulus value. *D,* oviposition frequency of zebrafish mating pairs is increased after exposure to 4-hydroxyphenylacetic acid, final concentrations as indicated. *Blue line* indicates control value (*left gray bar*). All three concentrations of 4-hydroxyphenylacetic acid are active, ***, $p < 0.001$. Naris closure (*right gray bar*) abolishes the increase in oviposition events, **, $p < 0.02$. *E,* schematic representation of the olfactory-mediated response of zebrafish mating pairs to 4-hydroxyphenylacetic acid.

receptors, and have been successful for ORA1, for which we identified and characterized several agonists.

We have shown ORA1 to be a highly sensitive and specific receptor for 4-hydroxyphenylacetic acid. An extensive search of structurally related compounds yielded no compound with similar or better potency and agonist efficacy. Albeit we cannot exclude the existence of structurally unrelated agonists, within the range of chemical structures analyzed, 4-hydroxyphenylacetic acid emerges as the optimal activator for ORA1. The best agonists among related compounds were about 10-fold less potent and exhibited less than two-thirds of the efficacy compared with 4-hydroxyphenylacetic acid. This large difference is consistent with the hypothesis that 4-hydroxyphenylacetic acid may be the physiologically relevant ligand for ORA1.

4-Hydroxyphenylacetic acid is detected by ORA1 with at least an order of magnitude higher sensitivity than typical food odors, such as amino acids (EC_{50} values between 10 and 100 μM *in vivo* (24, 26, 27)) or the death-signaling odor cadaverine (11), even though measurements in heterologous systems may exhibit lower sensitivities for odorants than are observed *in vivo* (see *e.g.* Refs. 28 and 29). This high sensitivity is consistent with a pheromonal function for 4-hydroxyphenylacetic acid, because pheromones are expected to be detected at lower concentrations than normal odorants (21).

4-Hydroxyphenylacetic acid is a biogenic compound, which occurs in several metabolic pathways including a minor catabolic pathway for tyrosine (transamination, decarboxylation, and oxidation of the resulting aldehyde to the corresponding

acid (*e.g.* Ref. 30 and Brenda-enzymes). 4-Hydroxyphenylacetic acid is produced in species as diverse as humans, insects, fungi, and bacteria (Refs. 31–34, respectively). It is present in micromolar concentrations in several bodily secretions including urine, feces (31), and saliva (35), and has been suggested as an antimicrobial agent (32–34), and also as component of a sexual display pheromone in felines (36).

Here we show that 4-hydroxyphenylacetic acid can modulate oviposition, a reproductive behavior, in zebrafish. This modulation appears to be mediated via the sense of smell, because it is abolished by naris closure. So far mostly various steroids and prostaglandins have been discussed as reproductive pheromones in fish species, but many pheromones remain unidentified up to now (22). We propose that 4-hydroxyphenylacetic acid may be in this category. Although we cannot exclude that 4-hydroxyphenylacetic acid may be mimicking a so far unknown endogenous steroid or prostaglandin, several known steroid and prostaglandin pheromones (21, 22) could not activate ORA1 in our assays.

ORA1 appears to be a plausible candidate for mediating the pheromonal effect of 4-hydroxyphenylacetic acid due to its high affinity and specificity. Further experiments will be required to firmly demonstrate this link and to rule out (or establish) the presence of other olfactory receptors for 4-hydroxyphenylacetic acid. Thus, the data presented here give a first glimpse onto a putative novel reproductive pheromone. Unfortunately, a thorough examination of this intriguing possibility is beyond the scope of the present study.

Currently, both the olfactory sensory neuron type, in which *ora1* is expressed, and its signal transduction mechanism are not known. Four morphologically and functionally different types of olfactory sensory neurons have been described so far in teleost fishes (37). Of these, crypt neurons can be excluded (38, 39), and ciliated neurons appear unlikely (39), which leaves the newly discovered kappe neurons (37) or microvillous neurons (39). The latter possibility would be analogous to the expression of *v1r* in microvillous neurons. Of the G proteins expressed in the olfactory epithelium of zebrafish (40), $G\alpha_i$ has been shown to correlate with crypt neurons (38, 39), and $G\alpha_{olf}$ is assumed to be specific for ciliated neurons, which leaves one of the two $G\alpha_o$ proteins expressed in zebrafish olfactory sensory neurons as possibilities (40).

Our results reported here, the high specificity of ORA1 toward 4-hydroxyphenylacetic acid, together with the low threshold of detection, and the activity of this odor in enhancing a reproductive function (Fig. 5*E*), are consistent with the hypothesis that 4-hydroxyphenylacetic acid may have a pheromone function in zebrafish, and thus suggest ORA1 as a potential pheromone receptor. It is intriguing to speculate that despite the drastic differences in the evolutionary dynamics of *v1r* and *ora* genes and notwithstanding the opposing requirements for odors posed by aquatic and terrestrial habitats, a function as pheromone receptor may be shared as well as ancestral for these two orthologous gene families.

Acknowledgments—We thank Ulrike Redel, Peggy Grossmann, and Mehmet Saltürk for excellent technical assistance. Luis Saraiva was involved in an early phase of this project.

REFERENCES

1. Leinders-Zufall, T., Ishii, T., Mombaerts, P., Zufall, F., and Boehm, T. (2009) Structural requirements for the activation of vomeronasal sensory neurons by MHC peptides. *Nat. Neurosci.* **12,** 1551–1558
2. Haga, S., Hattori, T., Sato, T., Sato, K., Matsuda, S., Kobayakawa, R., Sakano, H., Yoshihara, Y., Kikusui, T., and Touhara, K. (2010) The male mouse pheromone ESP1 enhances female sexual receptive behaviour through a specific vomeronasal receptor. *Nature* **466,** 118–122
3. Isogai, Y., Si, S., Pont-Lezica, L., Tan, T., Kapoor, V., Murthy, V. N., and Dulac, C. (2011) Molecular organization of vomeronasal chemoreception. *Nature* **478,** 241–245
4. Boschat, C., Pélofi, C., Randin, O., Roppolo, D., Lüscher, C., Broillet, M. C., and Rodriguez, I. (2002) Pheromone detection mediated by a V1r vomeronasal receptor. *Nat. Neurosci.* **5,** 1261–1262
5. Del Punta, K., Leinders-Zufall, T., Rodriguez, I., Jukam, D., Wysocki, C. J., Ogawa, S., Zufall, F., and Mombaerts, P. (2002) Deficient pheromone responses in mice lacking a cluster of vomeronasal receptor genes. *Nature* **419,** 70–74
6. Saraiva, L. R., and Korsching, S. I. (2007) A novel olfactory receptor gene family in teleost fish. *Genome Res.* **17,** 1448–1457
7. Venkatesh, B., Lee, A. P., Ravi, V., Maurya, A. K., Lian, M. M., Swann, J. B., Ohta, Y., Flajnik, M. F., Sutoh, Y., Kasahara, M., Hoon, S., Gangu, V., Roy, S. W., Irimia, M., Korzh, V., Kondrychyn, I., Lim, Z. W., Tay, B. H., Tohari, S., Kong, K. W., Ho, S., Lorente-Galdos, B., Quilez, J., Marques-Bonet, T., Raney, B. J., Ingham, P. W., Tay, A., Hillier, L. W., Minx, P., Boehm, T., Wilson, R. K., Brenner, S., and Warren, W. C. (2014) Elephant shark genome provides unique insights into gnathostome evolution. *Nature* **505,** 174–179
8. Friedrich, R. W. (2013) Neuronal computations in the olfactory system of zebrafish. *Annu. Rev. Neurosci.* **36,** 383–402
9. Bufe, B., Hofmann, T., Krautwurst, D., Raguse, J. D., and Meyerhof, W. (2002) The human TAS2R16 receptor mediates bitter taste in response to β-glucopyranosides. *Nat. Genet.* **32,** 397–401
10. Behrens, M., Brockhoff, A., Batram, C., Kuhn, C., Appendino, G., and Meyerhof, W. (2009) The human bitter taste receptor hTAS2R50 is activated by the two natural bitter terpenoids andrographolide and amarogentin. *J. Agric. Food Chem.* **57,** 9860–9866
11. Hussain, A., Saraiva, L. R., Ferrero, D. M., Ahuja, G., Krishna, V. S., Liberles, S. D., and Korsching, S. I. (2013) High-affinity olfactory receptor for the death-associated odor cadaverine. *Proc. Natl. Acad. Sci. U.S.A.* **110,** 19579–19584
12. Schack, H. B., Malte, H., and Madsen, P. T. (2008) The responses of Atlantic cod (*Gadus morhua* L.) to ultrasound-emitting predators: stress, behavioural changes or debilitation? *J. Exp. Biol.* **211,** 2079–2086
13. Meyerhof, W., Batram, C., Kuhn, C., Brockhoff, A., Chudoba, E., Bufe, B., Appendino, G., and Behrens, M. (2010) The molecular receptive ranges of human TAS2R bitter taste receptors. *Chem. Senses* **35,** 157–170
14. Ammon, C., Schäfer, J., Kreuzer, O. J., and Meyerhof, W. (2002) Presence of a plasma membrane targeting sequence in the amino-terminal region of the rat somatostatin receptor 3. *Arch. Physiol. Biochem.* **110,** 137–145
15. Kreuzer, O. J., Krisch, B., Déry, O., Bunnett, N. W., and Meyerhof, W. (2001) Agonist-mediated endocytosis of rat somatostatin receptor subtype 3 involves β-arrestin and clathrin coated vesicles. *J. Neuroendocrinol.* **13,** 279–287
16. Bufe, B., Breslin, P. A., Kuhn, C., Reed, D. R., Tharp, C. D., Slack, J. P., Kim, U. K., Drayna, D., and Meyerhof, W. (2005) The molecular basis of individual differences in phenylthiocarbamide and propylthiouracil bitterness perception. *Curr. Biol.* **15,** 322–327
17. Ueda, T., Ugawa, S., Yamamura, H., Imaizumi, Y., and Shimada, S. (2003) Functional interaction between T2R taste receptors and G-protein α subunits expressed in taste receptor cells. *J. Neurosci.* **23,** 7376–7380
18. Saito, H., Kubota, M., Roberts, R. W., Chi, Q., and Matsunami, H. (2004) RTP family members induce functional expression of mammalian odorant receptors. *Cell* **119,** 679–691
19. Loconto, J., Papes, F., Chang, E., Stowers, L., Jones, E. P., Takada, T., Kumánovics, A., Fischer Lindahl, K., and Dulac, C. (2003) Functional expression of murine V2R pheromone receptors involves selective associa-

tion with the M10 and M1 families of MHC class Ib molecules. *Cell* **112,** 607–618
20. Behrens, M., Bartelt, J., Reichling, C., Winnig, M., Kuhn, C., and Meyerhof, W. (2006) Members of RTP and REEP gene families influence functional bitter taste receptor expression. *J. Biol. Chem.* **281,** 20650–20659
21. Friedrich, R. W., and Korsching, S. I. (1998) Chemotopic, combinatorial, and noncombinatorial odorant representations in the olfactory bulb revealed using a voltage-sensitive axon tracer. *J. Neurosci.* **18,** 9977–9988
22. Stacey, N., and Sørensen, P. (2005) Reproductive pheromones. In *Behaviour and Physiology of Fish* (Sloman, K. A., Wilson, R. W., and Balshine, S., eds) pp. 359–412, Elsevier, Amsterdam
23. Yamamoto, Y., Hino, H., and Ueda, H. (2010) Olfactory imprinting of amino acids in lacustrine sockeye salmon. *PLoS One* **5,** e8633
24. Friedrich, R. W., and Korsching, S. I. (1997) Combinatorial and chemotopic odorant coding in the zebrafish olfactory bulb visualized by optical imaging. *Neuron* **18,** 737–752
25. Cao, Y., Oh, B. C., and Stryer, L. (1998) Cloning and localization of two multigene receptor families in goldfish olfactory epithelium. *Proc. Natl. Acad. Sci. U.S.A.* **95,** 11987–11992
26. Michel, W. C., and Lubomudrov, L. M. (1995) Specificity and sensitivity of the olfactory organ of the zebrafish, *Danio rerio*. *J. Comp. Physiol. A* **177,** 191–199
27. Fuss, S. H., and Korsching, S. I. (2001) Odorant feature detection: activity mapping of structure response relationships in the zebrafish olfactory bulb. *J. Neurosci.* **21,** 8396–8407
28. Mombaerts, P. (2004) Genes and ligands for odorant, vomeronasal and taste receptors. *Nat. Rev. Neurosci.* **5,** 263–278
29. Oka, Y., Katada, S., Omura, M., Suwa, M., Yoshihara, Y., and Touhara, K. (2006) Odorant receptor map in the mouse olfactory bulb: *in vivo* sensitivity and specificity of receptor-defined glomeruli. *Neuron* **52,** 857–869
30. Gossauer, A. (2006) *Struktur und Reaktivitaet der Biomolekuele: Eine Einfuehrung in die organische Chemie*, 1st ed., Helvetica Chimica Acta, Zurich
31. Li, M., Wang, B., Zhang, M., Rantalainen, M., Wang, S., Zhou, H., Zhang, Y., Shen, J., Pang, X., Zhang, M., Wei, H., Chen, Y., Lu, H., Zuo, J., Su, M., Qiu, Y., Jia, W., Xiao, C., Smith, L. M., Yang, S., Holmes, E., Tang, H., Zhao, G., Nicholson, J. K., Li, L., and Zhao, L. (2008) Symbiotic gut microbes modulate human metabolic phenotypes. *Proc. Natl. Acad. Sci. U.S.A.* **105,** 2117–2122
32. Dettner, K., and Schwinger, G. (1980) Defensive substances from pygidial glands of water beetles. *Biochem. Syst. Ecol.* **8,** 89–95
33. Ko, H. S., Jin, R. D., Krishnan, H. B., Lee, S. B., and Kim, K. Y. (2009) Biocontrol ability of Lysobacter antibioticus HS124 against Phytophthora blight is mediated by the production of 4-hydroxyphenylacetic acid and several lytic enzymes. *Curr. Microbiol.* **59,** 608–615
34. Ohtani, K., Fujioka, S., Kawano, T., Shimada, A., and Kimura, Y. (2011) Nematicidal activities of 4-hydroxyphenylacetic acid and oidiolactone D produced by the fungus *Oidiodendron* sp. *Z. Naturforsch C* **66,** 31–34
35. Takahama, U., Oniki, T., and Murata, H. (2002) The presence of 4-hydroxyphenylacetic acid in human saliva and the possibility of its nitration by salivary nitrite in the stomach. *FEBS Lett.* **518,** 116–118
36. Pageat, P., and Gaultier, E. (2003) Current research in canine and feline pheromones. *Vet. Clin. North Am. Small Anim. Pract.* **33,** 187–211
37. Ahuja, G., Nia, S. B., Zapilko, V., Shiriagin, V., Kowatschew, D., Oka, Y., and Korsching, S. I. (2014) Kappe neurons, a novel population of olfactory sensory neurons. *Sci. Rep.* **4,** 4037
38. Ahuja, G., Ivandic, I., Saltürk, M., Oka, Y., Nadler, W., and Korsching, S. I. (2013) Zebrafish crypt neurons project to a single, identified mediodorsal glomerulus. *Sci. Rep.* **3,** 2063
39. Oka, Y., Saraiva, L. R., and Korsching, S. I. (2012) Crypt neurons express a single V1R-related *ora* gene. *Chem. Senses* **37,** 219–227
40. Oka, Y., and Korsching, S. I. (2011) Shared and unique G alpha proteins in the zebrafish *versus* mammalian senses of taste and smell. *Chem. Senses* **36,** 357–365